Metabolism 161 (2024) 156034

Contents lists available at ScienceDirect

Metabolism

journal homepage: www.journals.elsevier.com/metabolism

Inter-organ cross-talk in human cancer cachexia revealed by spatial metabolomics

Na Sun [a,1], Tanja Krauss [b,1], Claudine Seeliger [b,c], Thomas Kunzke [a], Barbara Stöckl [a,b], Annette Feuchtinger [a], Chaoyang Zhang [a], Andreas Voss [a], Simone Heisz [b], Olga Prokopchuk [d], Marc E. Martignoni [d], Klaus-Peter Janssen [d], Melina Claussnitzer [e,f,g,h], Hans Hauner [b,c,i,2,*], Axel Walch [a,2,*]

[a] Research Unit Analytical Pathology, Helmholtz Zentrum München, Neuherberg, Germany
[b] Else Kröner Fresenius Center for Nutritional Medicine, School of Life Sciences, Technical University of Munich, Freising-Weihenstephan, Germany
[c] ZIEL Institute for Food and Health, Technical University of Munich, Freising-Weihenstephan, Germany
[d] Department of Surgery, Klinikum rechts der Isar, University Hospital of the Technical University of Munich, Munich, Germany
[e] The Novo Nordisk Foundation Center for Genomic Mechanisms of Disease, Broad Institute of MIT and Harvard, Cambridge, MA 02142, USA
[f] Diabetes Unit and Center for Genomic Medicine, Massachusetts General Hospital, Boston, MA 02114, USA
[g] Institute of Nutritional Science, University of Hohenheim, 70599 Stuttgart, Germany
[h] Department of Medicine, Harvard Medical School, Boston, MA, USA
[i] Institute of Nutritional Medicine, School of Medicine, Technical University of Munich, Munich, Germany

ARTICLE INFO

Keywords:
Cancer cachexia patients
Spatial metabolomics
Inter-organ cross-talk
Machine learning
Metabolomics classifier
Diagnostics of cachexia

ABSTRACT

Background: Cancer cachexia (CCx) presents a multifaceted challenge characterized by negative protein and energy balance and systemic inflammatory response activation. While previous CCx studies predominantly focused on mouse models or human body fluids, there's an unmet need to elucidate the molecular inter-organ cross-talk underlying the pathophysiology of human CCx.

Methods: Spatial metabolomics were conducted on liver, skeletal muscle, subcutaneous and visceral adipose tissue, and serum from cachectic and control cancer patients. Organ-wise comparisons were performed using component, pathway enrichment and correlation network analyses. Inter-organ correlations in CCx altered pathways were assessed using Circos. Machine learning on tissues and serum established classifiers as potential diagnostic biomarkers for CCx.

Results: Distinct metabolic pathway alteration was detected in CCx, with adipose tissues and liver displaying the most significant ($P \leq 0.05$) metabolic disturbances. CCx patients exhibited increased metabolic activity in visceral and subcutaneous adipose tissues and liver, contrasting with decreased activity in muscle and serum compared to control patients. Carbohydrate, lipid, amino acid, and vitamin metabolism emerged as highly interacting pathways across different organ systems in CCx. Muscle tissue showed decreased ($P \leq 0.001$) energy charge in CCx patients, while liver and adipose tissues displayed increased energy charge ($P \leq 0.001$). We stratified CCx patients by severity and metabolic changes, finding that visceral adipose tissue is most affected, especially in cases of severe cachexia. Morphometric analysis showed smaller ($P \leq 0.05$) adipocyte size in visceral adipose tissue, indicating catabolic processes. We developed tissue-based classifiers for cancer cachexia specific to individual organs, facilitating the transfer of patient serum as minimally invasive diagnostic markers of CCx in the constitution of the organs.

Conclusions: These findings support the concept of CCx as a multi-organ syndrome with diverse metabolic alterations, providing insights into the pathophysiology and organ cross-talk of human CCx. This study pioneers spatial metabolomics for CCx, demonstrating the feasibility of distinguishing cachexia status at the organ level using serum.

* Corresponding authors.
E-mail addresses: hans.hauner@tum.de (H. Hauner), axelkarl.walch@helmholtz-munich.de (A. Walch).
[1] These authors contributed equally to this work.
[2] Shared senior authorship.

https://doi.org/10.1016/j.metabol.2024.156034
Received 19 April 2024; Accepted 12 September 2024
Available online 17 September 2024

1. Introduction

Cancer cachexia (CCx) is a complex, multifactorial disorder occurring in 50–80 % of patients with cancer and is responsible for >20 % of cancer-related deaths [1,2]. Patients with cancers of the gastrointestinal tract, such as pancreatic, gastric, or colorectal cancers, are frequently affected by CCx [3]. Chronic inflammation and weight loss due to wasting of fat and muscle mass are central hallmarks of CCx [4]. Signals released by the tumor, the tumor microenvironment, and distant tissues such as the liver, gut, inflammatory system, and brain in patients with CCx affect adipose and muscle tissues and other organs including the heart and circulatory system [5]. The derangement and wasting of adipose tissue in CCx is characterized by activated lipolysis and increased release of free fatty acids. In addition, breakdown of muscle protein in CCx leads to the release of amino acids, which, along with inflammatory cytokines such as IL-6, TNF-α, and IL-1β, induces the secretion of acute-phase proteins from the liver [1,5]. These effects and crosstalk signals between organs all contribute to systemic inflammation, sarcopenia, anorexia, hypermetabolism, metabolic dysregulation, and tissue wasting in patients with CCx [6–8].

Metabolomics is being increasingly applied to study the metabolic alterations in CCx, mainly using murine cancer models [9]. For example, an analysis of mouse serum and muscle tissue identified significant alterations in lipid and energy metabolism in a murine model of cancer-induced cachexia, including early reductions in amino acids, progressive decreases in short-chain acylcarnitines, changes in lipoprotein profiles, and shifts in phospholipid concentrations [10]. Aerobic and resistance training have shown to induce skeletal muscle plasticity in the colon-26 murine model of cancer cachexia, indicating potential therapeutic avenues targeting muscle metabolism [11]. In humans, mass spectrometry-based metabolomics studies of plasma from patients with and without CCx have revealed some relevant deviations. In one such study, Cala et al. found that patients with CCx had increased plasma levels of cortisol and decreased plasma levels of glycerophospholipids, sphingolipids, and amino acids and their derivatives, especially arginine, tryptophan, indolelactic acid, and threonine [12]. In another study, Miller et al. found that a plasma profile of lysophosphatidylcholines, L-Proline, hexadecanoic acid, octadecanoic acid, and phenylalanine was highly discriminative of weight loss in patients with CCx [13]. Furthermore, recent findings have underscored the critical role of metabolic dysregulation in cancer cachexia. For instance, a study highlighted that specific metabolic signatures in CCx are associated with alterations in lipid metabolism and mitochondrial function in skeletal muscle tissue, which may contribute to the characteristic wasting syndrome observed in CCx patients [14]. Additionally, another study emphasized the importance of understanding metabolic alterations across different tissues, suggesting that multi-organ approaches could provide comprehensive insights into CCx pathophysiology [15]. The critical role of whole-body lipolysis in human CCx has been well-documented, demonstrating increased rates of lipolysis and free fatty acid release, further contributing to the energy imbalance and muscle wasting observed in these patients [16].

There have been few metabolite analyses of tissues other than blood from patients with CCx. In a previous study, we used matrix-assisted laser desorption/ionization (MALDI) mass spectrometry imaging (MSI) to explore metabolic changes in CCx in a murine cancer model complemented by human patients [17]. This method enables the spatially resolved visualization of metabolites in biological tissue specimens and quantitative study of metabolic dynamics in situ [17,18]. We found that skeletal muscle tissues of cachectic mice and patients with CCx had increased quantities of lysine, arginine, proline, and tyrosine and reduced quantities of glutamate and aspartate [17]. Beyond the changes in amino acid metabolism, we also observed a decreased energy charge in cachectic mouse muscle tissues [17]. Energy charge is a measure of the cell's energetic status, defined as the ratio of adenylate energy forms (ATP, ADP, and AMP), which reflects the balance between ATP production and consumption [19]. This decrease in energy charge indicates significant disruptions in energy metabolism, further underscoring the metabolic alterations characteristic of cancer cachexia [14]. Because CCx is a multi-organ syndrome, a systematic approach targeting metabolic changes in multiple tissues simultaneously is more appropriate than investigating a single tissue or body fluid in isolation.

Here, we demonstrate for the first time a multi-organ spatial metabolomics approach to detect metabolic alterations in the liver, skeletal muscle, subcutaneous and visceral adipose tissues, and serum of patients with CCx. Our comprehensive tissue-based datasets from various organ systems of CCx cancer patients and control cancer patients reveal significant metabolic differences between these patient groups. We assessed their suitability for diagnostic classification using machine learning techniques and explored the potential of tissue-based metabolic classifiers as serum markers.

2. Material and methods

2.1. Patient cohort and sample collection

The study was approved by the Ethics Committee of the Medical Faculty of the Technical University of Munich (project number 409/16 S) and is registered under "*Deutsches Register Klinischer Studien*" (DRKS00017285). All patients provided written informed consent before participation in this study and the whole handling complies with the Declaration of Helsinki. The study's overall workflow performance is illustrated in Fig. 1.

Samples of liver (from liver segments III, IVb or V where macroscopically no liver lesions were seen), musculus rectus abdominis, visceral fat from the greater omentum, and subcutaneous fat were collected (75 samples in total) from a total of 15 patients with malignant diseases of the gastrointestinal tract (10 with CCx and five control patients) during surgical procedures at the Department of Surgery, *Klinikum rechts der Isar* (University Hospital of the TUM). Upon recruitment prior to surgery, patients' clinical characteristics were collected through standardized questionnaires, anthropometry, routine clinical chemistry, and medication (Supplementary Tables 1–2). Skeletal muscle area index, a marker of sarcopenia, was evaluated in all patients as described previously [20,21]. The 10 patients with CCx had a history of >5 % weight loss during the 6 months prior to surgery, which is in accordance with the international consensus on CCx diagnosis [22]. The control group comprised five cancer patients who had experienced weight loss of <5 % over the same period. Two of these patients lost over 2 % of their weight and presented with sarcopenia; however, they were included in the control group because our study focused on weight loss as the primary indicator of cancer cachexia. Previous studies have shown significant survival outcomes linked to 5 % and 10 % weight loss thresholds in colorectal and pancreatic cancer patients [21,23], highlighting weight loss as a critical prognostic marker.

2.2. MALDI-FTICR mass spectrometry imaging

Liver, muscle, and adipose tissues were sectioned into 12 μm in a cryostat (CM1950, Leica Microsystems, Wetzlar, Germany) according to previous protocols [17,24].

A matrix solution of 10 mg/ml 9-aminoacridine (9AA) hydrochloride monohydrate (Sigma-Aldrich, Germany) in water/methanol 30:70 (*v*/v) was applied using a SunCollect™ automatic sprayer (Sunchrom, Friedrichsdorf, Germany). 9AA was selected for its ability to mitigate matrix interferences in the low-mass range, thereby enhancing sensitivity and ensuring linear detection across a wide spectrum of low-molecular-weight metabolites. Previous studies have robustly demonstrated the effectiveness of 9-AA in negative ion mode, underscoring its suitability for our metabolomic approach [25,26]. The MALDI-FTICR MSI measurement was conducted according to established methods [27–29] using a Bruker Solarix 7T FT-ICR-MS (Bruker Daltonik, Bremen, Germany) in negative ion mode, involving 100 laser shots at a 1000 Hz

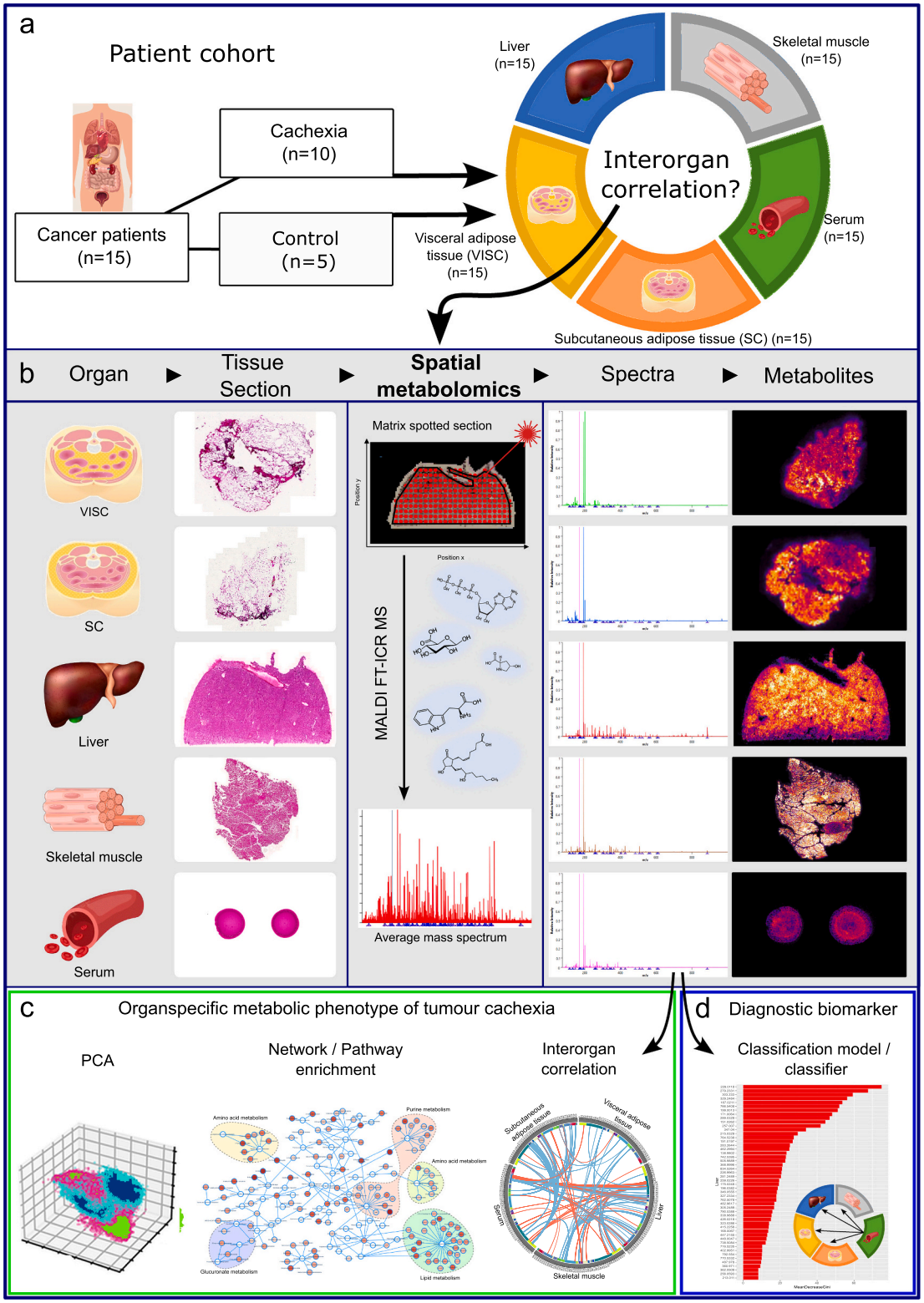

Fig. 1. Workflow of spatial metabolomics for studying inter-organ cross-talk in human cancer cachexia.
a: Samples of subcutaneous and visceral adipose tissue, liver, muscle, and serum from 10 cachectic and five control patients with cancer were investigated with MALDI-MSI to detect differences in individual metabolomes and inter-organ cross-talk related to cancer cachexia.
b: MALDI-MSI workflow including tissue sectioning, spatial metabolomics using high mass resolution MALDI-FT-ICR MS imaging, mass spectra acquisition, and data processing including peak picking and metabolite annotation.
c: Mass spectra of individual organs underwent unsupervised principal component analysis (PCA), metabolic correlation analysis, and inter-organ correlation analysis.
d: Classification models were generated using the Random Forest-based machine learning algorithm.

frequency. Data were acquired over the mass range of *m/z* 75–1000 with a 50 μm lateral resolution. Mass spectrometry peaks were annotated using the Human Metabolome Database (HMDB, https://www.hmdb.ca/) [30], METASPACE (https://metaspace2020.eu) [31], and the KEGG database (https://www.genome.jp/kegg/) [32] (Supplementary methods, Supplementary Table 3).

2.3. Data analysis

Metabolic correlation networks were created with Cytoscape (v. 3.9.1) [33]. Nodes represent metabolites with a node size and color corresponding to the intensity log2 fold change between CCx and control patients. Edges represent pathway correlations. Metabolites with significant differences between CCx and control patients ($P \leq 0.05$) are shown. The network was visualized using the Compound Spring Embedder layout.

The mass spectra were subjected to unsupervised principal components analysis (PCA) using Python v. 3.8 to reduce the dimensionality of the data and to identify the principal components that explained the majority of the variance in the data. The data were first log-transformed and auto scaled to standardize the data across samples.

Energy charge is calculated as the ratio of the concentrations of ATP, ADP, and AMP as previously descript.[17] Quantitative morphometric analysis of visceral and subcutaneous adipose tissues was performed on H&E stained sections using an AxioScan 7 digital slide scanner (Zeiss, Jena, Germany) equipped with a 20× magnification objective. Image analysis was conducted using the Visiopharm software (Visiopharm, Hoersholm, Denmark), as previously described [34,35].

A nonparametric Mann-Whitney *U* test (Python v. 3.8, sci-kit v. 0.23.2) was performed to identify molecules that differed significantly between CCx and control patients. In all calculations, *m/z* values with a P-value <0.05 were considered statistically significant. The significantly altered molecules were used to perform pathway analyses using MetaboAnalyst 4.0 (https://www.metaboanalyst.ca/). In addition, Spearman's rank correlation was performed (Python v. 3.8, SciPy 1.2.0) to compare measured metabolites between organs. Unique significant correlations in the cachectic patients were visualized using Circos (v. 0.69.8). Pathway information for each metabolite was extracted from the KEGG database (https://www.genome.jp/kegg/).

Random Forest (RF) was employed to develop a classification and prediction model (R 4.3.1). The RF classifier was constructed using a dataset comprising 2000 randomly selected data points from each organ and the serum. The significance of each metabolite was assessed and ranked based on the Gini coefficient within the RF classifier. The top 50 metabolites, identified as the most influential, were subsequently utilized to construct and train the RF classifier based on the already selected 2000 data points. To evaluate the robustness and predictive performance of the trained RF classifier, a separate dataset consisting of 1000 randomly selected data points independent from the training set was employed for validation. The prediction accuracy, sensitivity, and specificity metrics were then calculated and reported. In the subsequent phase of our analysis, we developed a classifier exclusively composed of metabolites shared between the serum and the specific organs. This organ-specific classifier was subsequently applied to the serum dataset. In the final step, we established a comprehensive classifier, incorporating metabolites that demonstrated commonality across both serum and all organs, including the liver, skeletal muscle, subcutaneous adipose tissue, and visceral adipose tissue. This extended classifier was then employed for the analysis of the serum dataset.

3. Results

3.1. Multi-organ metabolic constitution revealed a clear separation between cachectic and control patients

Metabolic data revealed significant differences ($P \leq 0.05$) between cachectic and control cancer patients in all organ systems. Fig. 2a showed representative visualizations of distinct metabolites in liver and muscle sections. An unsupervised PCA analysis was performed to structure the metabolites among all 15 patients according to similarities and variances. The data were visualized in score plots separately for the visceral adipose tissue, subcutaneous adipose tissue, liver, muscle, and serum. The metabolic patterns of control patients formed a tight cluster, whereas those of CCx patients were more widely dispersed, highlighting a pronounced metabolic distinction between the two groups (Fig. 2b–f).

3.2. Adipose tissues and liver displayed the most metabolic alterations associated with cachexia

We identified 6135 *m/z* species (metabolites) across these organs and serum samples. Significant metabolic differences ($P \leq 0.05$) were observed between patients with CCx and control patients (Fig. 2b–f). In visceral adipose (Fig. 2b), subcutaneous adipose (Fig. 2c), and liver (Fig. 2d), a greater number of metabolites exhibited increases in CCx patients compared to control patients (visceral adipose: 1852 increased vs. 124 decreased in CCx; subcutaneous adipose: 1662 increased vs. 392 decreased in CCx; liver: 392 increased vs. 208 decreased in CCx). Conversely, muscle (Fig. 2e) and serum (Fig. 2f) showed the opposite pattern, with more metabolites decreased in the patients with CCx relative to the control patients (muscle: 84 increased vs. 170 decreased in CCx; serum: 56 increased vs. 101 decreased in CCx). Thus, liver and adipose tissues exhibited increased metabolic activity associated with cachexia, whereas the serum and muscle showed the opposite trend.

3.3. Correlation network analysis

We constructed metabolic correlation networks using Cytoscape based on pathway interactions in the liver, subcutaneous adipose, visceral adipose tissues, muscle, and serum, respectively (Figs. 3–4, Supplementary Figs. 1–5). Liver and adipose tissues displayed the most metabolic alterations associated with cachexia and revealed intensive network correlations (Figs. 3, 4), whereas only a few network associations were found in muscle tissue (Supplementary Fig. 4).

Fig. 3 shows the results of metabolic network analysis in the liver of CCx versus control patients. The overall network shows that most metabolites are increased in CCx. The representative visualizations of significantly altered pathways with high impact are highlighted in the correlation network analysis by color coding (Fig. 3). It is evident that nucleotide metabolism, amino acid metabolism, and arachidonic acid metabolism are highly upregulated in CCx liver compared with control patients. In contrast, inositol phosphate metabolism, ascorbate and aldarate metabolism, and pentose and glucuronate interconversions are significantly downregulated in CCx liver.

Comparison of interaction networks of subcutaneous adipose and visceral adipose is shown in Fig. 4. The resulting visualizations (Fig. 4a, b) reveal significant differences in the pathway correlations of the two networks. The majority of correlated pathways in the network of subcutaneous adipose are decreased in CCx, whereas in visceral adipose, the dominant pathways in the network are upregulated. In particular, arachidonic acid metabolism and metabolism of unsaturated fatty acids are highly downregulated in subcutaneous adipose, whereas a significant increase of these pathways is observed in visceral adipose. In addition, we observe perturbations in tryptophan metabolism, pyrimidine metabolism, and purine metabolism in both adipose tissues (Fig. 4).

3.4. Metabolic pathways were substantially disrupted in CCx

In total, 53 metabolic pathways were significantly ($P \leq 0.05$) altered between the patients with CCx and the control patients (Fig. 5a). Pathways for lipid, carbohydrate, and amino acid metabolism were the most affected by CCx. Other pathways contributing to metabolic changes in CCx included pathways for cofactor and vitamin metabolism, nucleotide

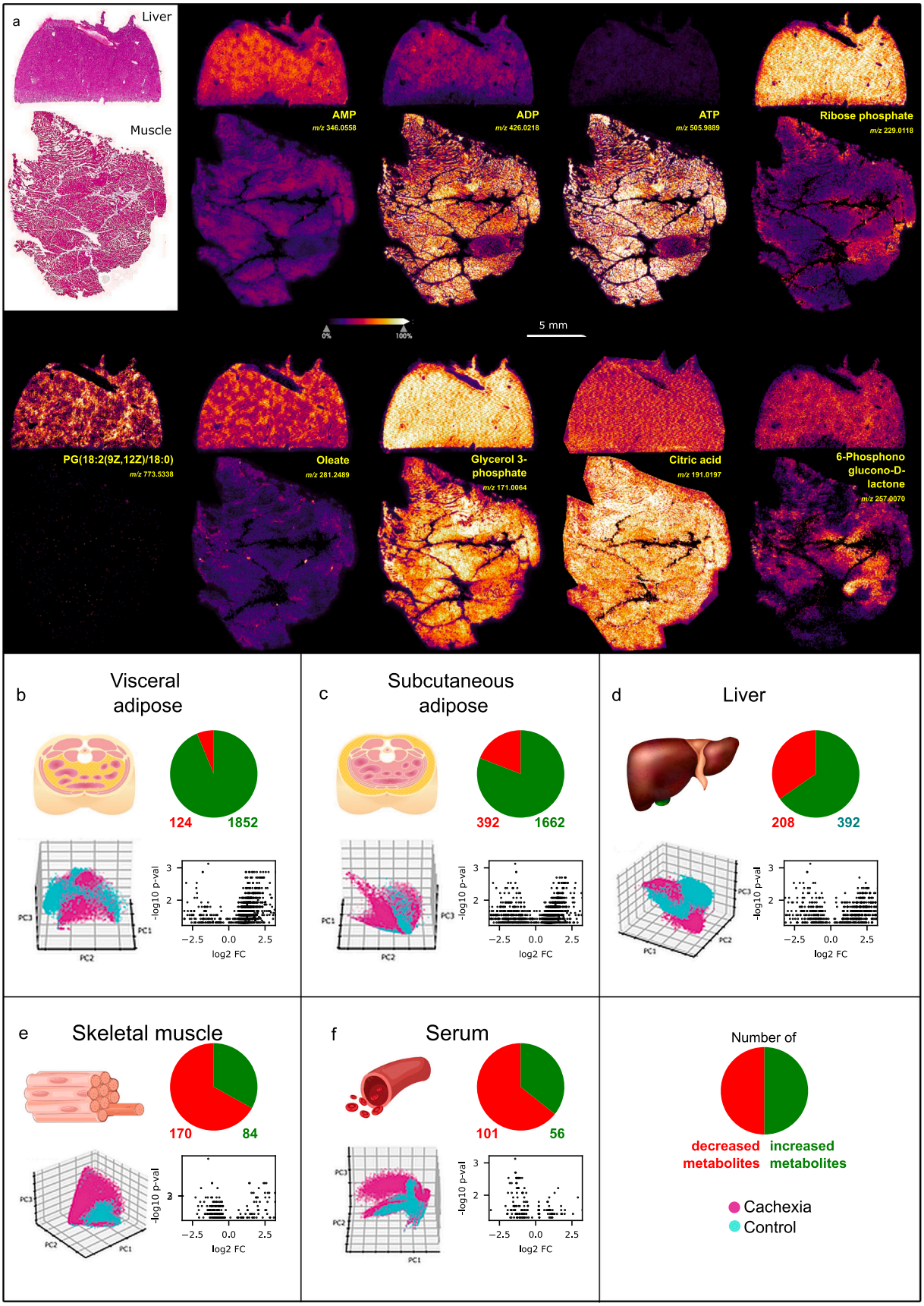

(caption on next page)

Fig. 2. Metabolic data revealed a clear separation between cachectic and control cancer patients.
a: representative visualization and intensity distribution maps of distinct metabolites in liver and muscle sections from one control cancer patient are shown. AMP, ADP, and ATP exhibit a gradually decreasing intensity in the liver. In contrast, a significant increase from AMP to ATP is observed in muscle tissue. Ribose phosphate, PG(18:2(9Z,12Z)/18:0), and oleate, which are classified as fatty acid and lipid, are more abundant in the liver, whereas citric acid from tricarboxylic acid cycle (TCA) cycle represents higher abundance in muscle tissue. Glycerol-3-phosphate and 6-Phosphono glucono-D-lactone, as intermediates in the glycolysis metabolic pathway and pentose phosphate pathway represent similar abundances in liver and muscle tissue.
b–f: Score plots were generated from unsupervised Principal Component Analysis (PCA) which clearly separates control and cachectic patients in serum, liver, muscle, subcutaneous adipose, and visceral adipose tissues. Volcano plots show the fold change of significantly altered metabolites, calculated by dividing the mean intensity of cachectic patients by the mean intensity of control patients. The pie charts depict the number of significantly decreased and increased metabolites in each tissue type. In subcutaneous adipose, visceral adipose tissues, and liver, more metabolites were increased in patients with CCx relative to control patients than vice versa. Muscle and serum showed the opposite pattern, with more metabolites decreased in patients with CCx relative to control patients than vice versa. PC: principal component; FC = fold change; p-val = P-value.

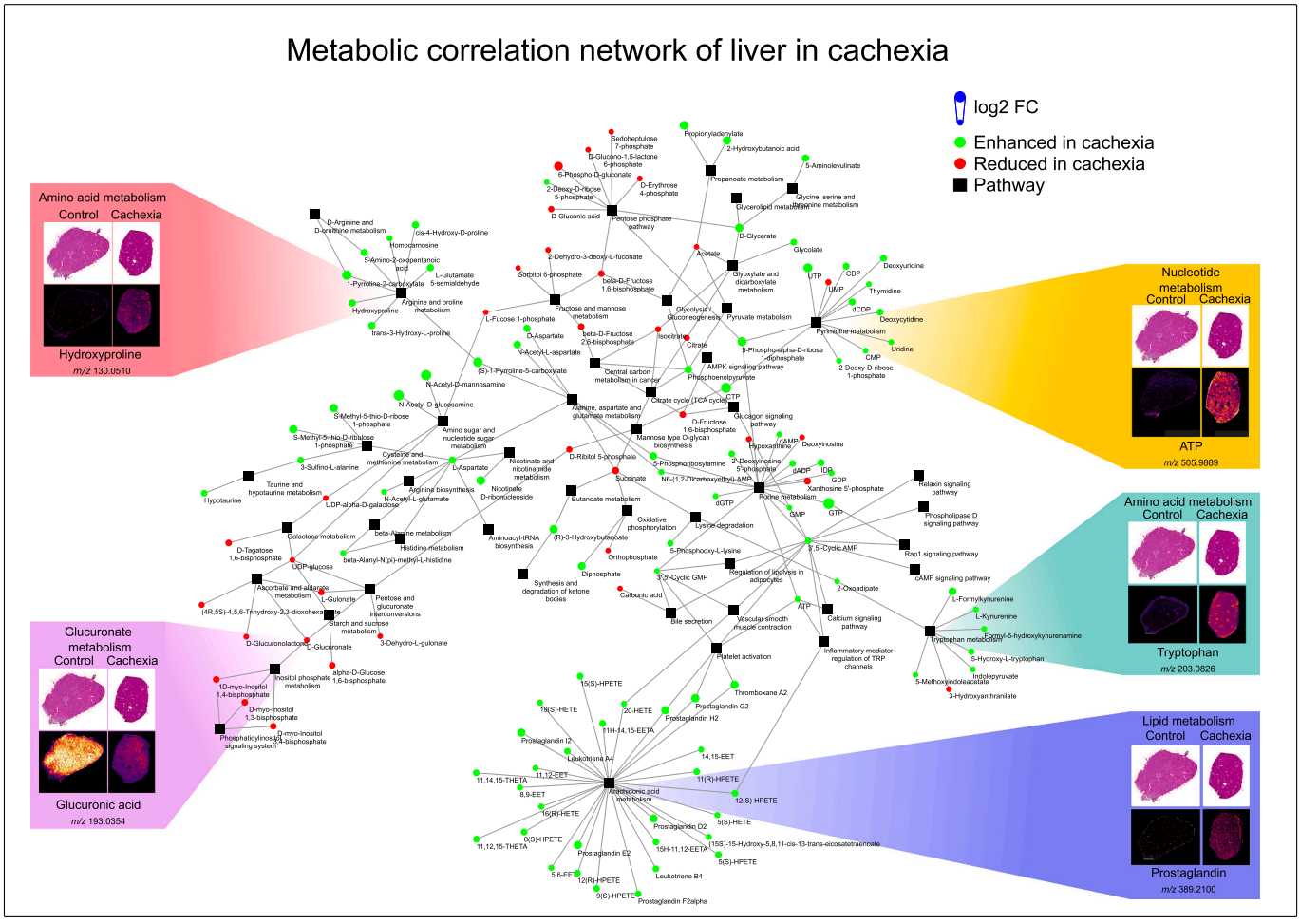

Fig. 3. Metabolic correlation network of liver in cachexia compared with control patients.
The network shows the correlation between different metabolites in liver cachexia compared with control patients, with nodes representing metabolites and edges representing KEGG pathway correlation between them. Node size is proportional to the log2 fold change. The nodes are colored based on log2 fold change. Green nodes represent value of 1 or greater for upregulation. Red nodes represent −1 or less for downregulation. The representative visualizations of significantly altered pathways with high impact are circled with a colored cloud. The intensity distribution maps of distinct metabolites from representative pathways in cachexia and control liver are as follows: ATP, tryptophan, prostaglandin, hydroxyproline, and glucuronic acid. The network was generated using Cytoscape software. (For interpretation of the references to color in this figure legend, the reader is referred to the web version of this article.)

metabolism, energy metabolism, and translation. Each organ displayed specific pathway changes in CCx. The liver contained the most altered pathways, followed by adipose tissues, then serum, and finally muscle (Fig. 5a).

3.5. *Distinct energy charges are observed in the adipose, liver, and muscle tissues in CCx*

We calculated the energy charge in adipose, liver, and muscle, respectively (Fig. 5b). Generally, the energy charge is higher in muscle (Median EC: 0.45) and adipose tissues (subcutaneous adipose Median EC: 0.43, visceral adipose Median EC: 0.47) than in the liver (Median EC: 0.25). We found a significant decrease ($P \leq 0.001$) in energy charge in CCx in muscle tissue. Furthermore, a significant increase ($P \leq 0.001$) in energy charge in CCx was detected in the liver, subcutaneous adipose, and visceral adipose tissues compared to the control patient groups (Fig. 5b).

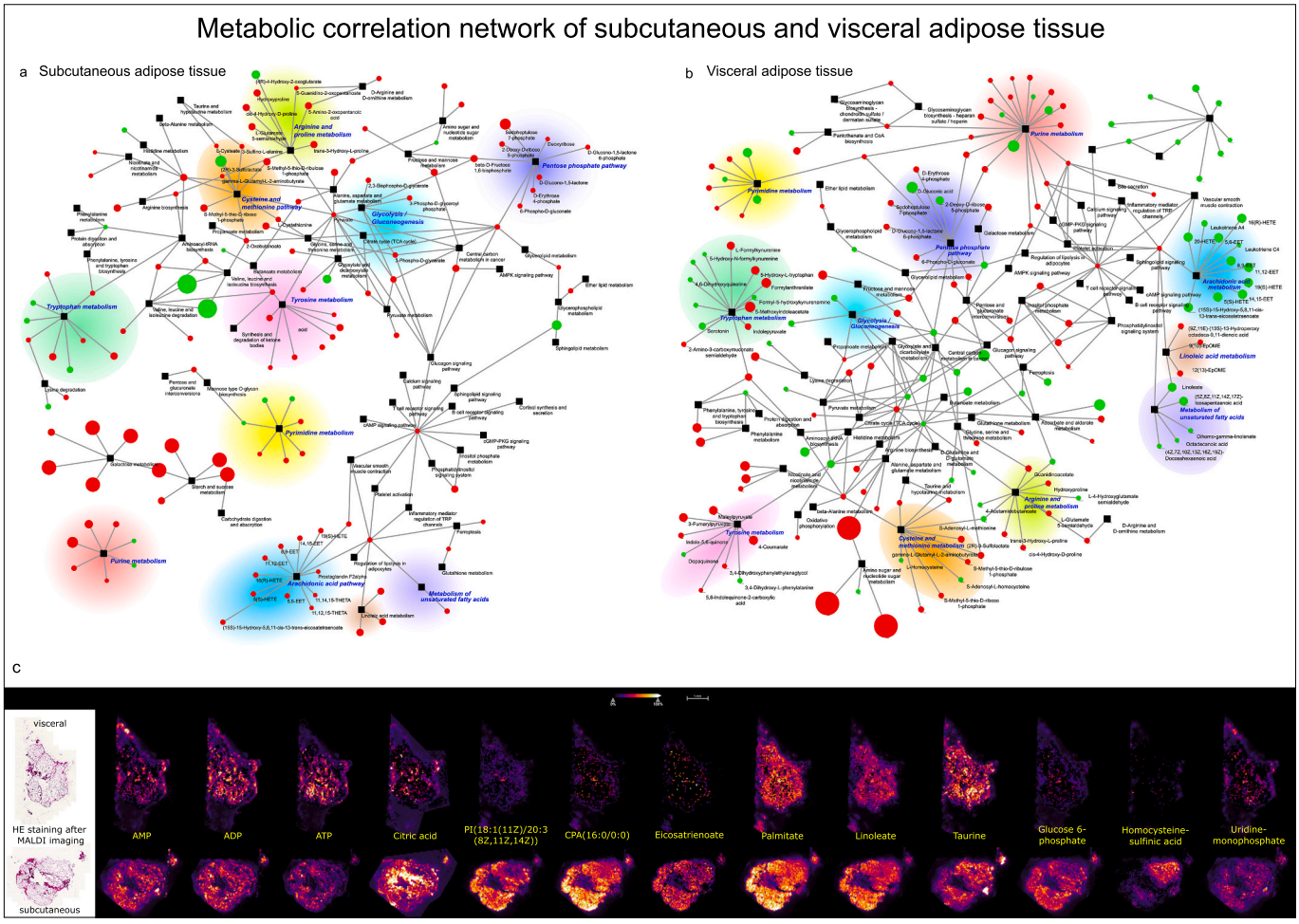

Fig. 4. Comparison of correlation networks of subcutaneous adipose and visceral adipose in cancer cachexia.
a, b: The network shows the correlation between different metabolites in cachexia compared with control patients, with nodes representing metabolites and edges representing KEGG pathway correlation between them. Node size is proportional to the log2 fold change. The nodes are colored based on log2 fold change. Green nodes represent value of 1 or greater for upregulation. Red nodes represent −1 or less for downregulation. Subcutaneous adipose (a) and visceral adipose (b) reveal significant differences in the pathway correlations networks. The representative visualization of selected pathways is circled with a colored cloud. c: Intensity distribution maps of example metabolites in subcutaneous and visceral adipose tissues of one cachexia patient are as follows: AMP (*m/z* 346.0558), ADP (m/z 426.0218), ATP (m/z 505.9889), citric acid (m/z 191.0197), PI(18:1(11Z)/20:3 (8Z,11Z,14Z)) (m/z 885.5498), CPA(16:0/0:0) (m/z 391.2255), eicosatrienoate (m/z 305.2486), palmitate (m/z 255.2330), linoleate (m/z 279.2331), taurine (m/z 124.0074), glucose 6-phosphate (m/z 259.0226), homocysteinesulfinic acid (m/z 166.0179), and uridine-monophosphate (m/z 323.0286). (For interpretation of the references to color in this figure legend, the reader is referred to the web version of this article.)

3.6. Patient stratification according to cachexia severity

We categorized patients into groups and assessed organ-specific metabolic changes in relation to the severity of cachexia. Specifically, we divided cachexia patients into two subgroups: 'Cachexia >5–10 % weight loss' and 'Cachexia >10 % weight loss'. When comparing all cachexia patients with the control group, we observed the most significant metabolic changes in adipose tissue (with significantly changed metabolites of 41 % in subcutaneous adipose and 39 % in visceral adipose), followed by the liver (12 %), muscle (5 %), and serum (3 %) (Fig. 5c). However, when examining changes in patients with the most substantial weight loss, it became evident that the significant metabolic alterations in cases of severe cachexia were predominantly found in visceral adipose tissue (with 59 % significantly changed metabolites), while changes in subcutaneous adipose tissue exhibited a dramatic decrease to 9 % (Fig. 5c).

3.7. Quantitative morphometric analysis of visceral and subcutaneous adipose tissues

We performed an image-based evaluation of adipocyte size on H&E-stained histological sections of visceral and subcutaneous adipose tissues from cachexia patients and control subjects (Fig. 6a). Our analysis reveals that adipocytes in visceral adipose tissue exhibit a significantly smaller cell size compared to control tissue ($P \leq 0.05$). Considering the observed reduction in cell size and the pronounced metabolic processes, these changes indicate a catabolic state. In subcutaneous adipose tissue, we did not observe significant changes in adipocyte size in cachectic conditions.

3.8. Specific pathways revealed inter-organ cross-talk in human CCx

The interactions between different metabolic pathways in CCx in the liver, muscle, adipose tissues, and serum are visualized with a circos plot. Specific pathways for carbohydrate, lipid, amino acid, and vitamin metabolism displayed correlations across organ systems in the patients with CCx (Fig. 6b). The liver exhibited the most pathway correlations with other organs. Most metabolic pathway association was found between liver and muscle. Remarkably, there are fewer connections between subcutaneous and visceral adipose tissues. Subcutaneous adipose tissue and visceral adipose tissue interacted with other organs in very

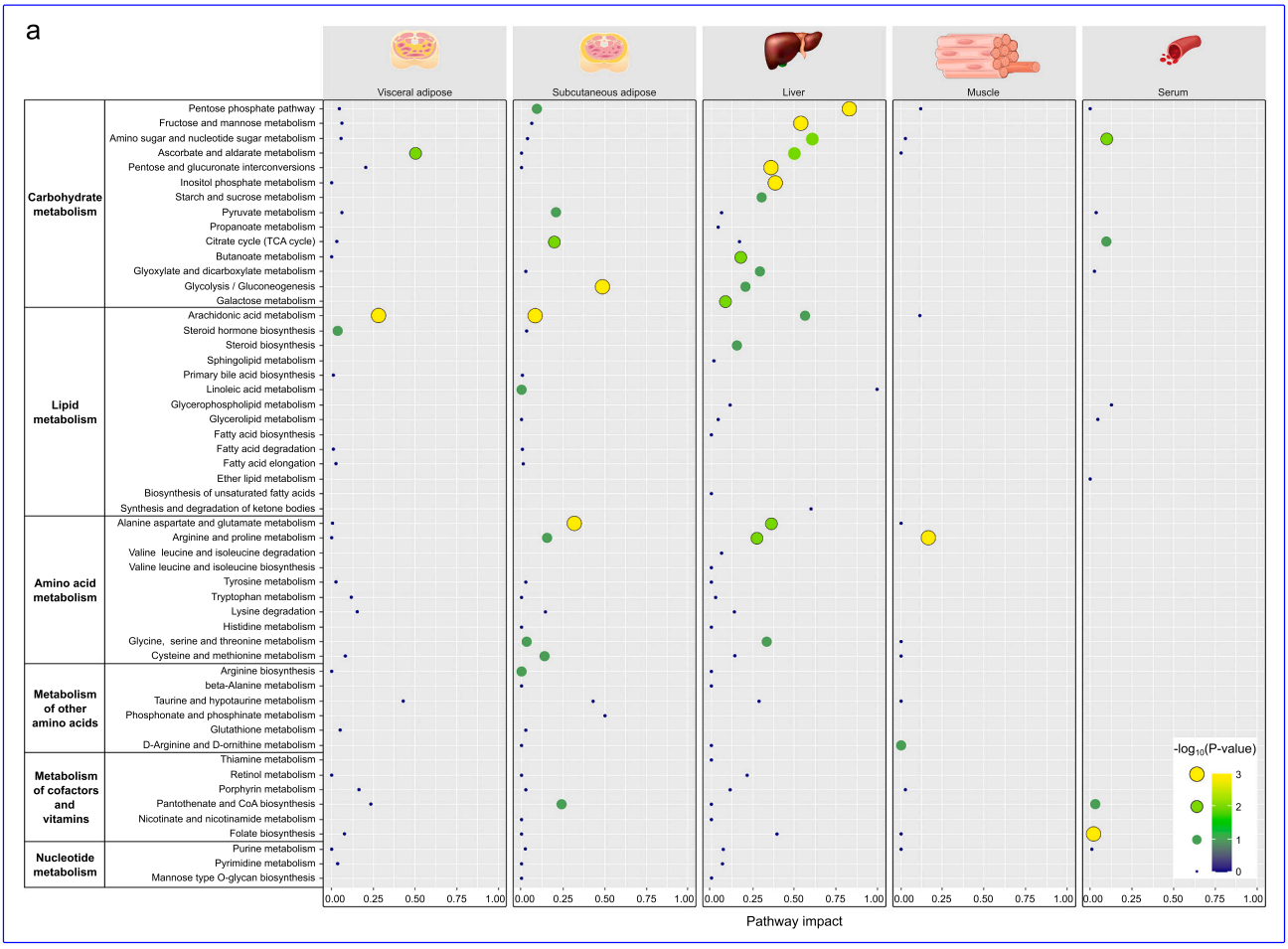

(caption on next page)

Fig. 5. Pathway enrichment analysis, energy charge in cancer cachexia and patient stratification according to cachexia severity.
a: Bubble plot presenting the pathway impact from MetaboAnalyst and the corresponding P value of each significantly altered pathway in cachexia. In total, 53 pathways were found to be altered in cachexia in individual tissues. The x-axis shows the pathway impact from MetaboAnalyst. The size and color of the bubbles represent the P-value.
b: Energy charge (EC) revealed a significantly charge in cachectic compared with control in subcutaneous adipose, visceral adipose, liver, and muscle tissues. Whiskers of the boxplots represent the lowest and highest peak intensities in each group. AMP, ADP, and ATP distribution in cachectic and non-cachectic muscle tissues are shown as example. *** $P \leq 0.001$, EC: energy charge.
c: Pie diagrams illustrated organ-specific metabolic changes in relation to the severity of cancer cachexia. Subgroups were formed for 'Cachexia > 5–10 % weight loss' and 'Cachexia > 10 % weight loss' to investigate organ-specific metabolic changes based on cachexia severity. When compared with the control group, the most significant metabolic changes were predominantly observed in visceral adipose tissue in cases of severe cachexia. As an example, we presented a visualization of taurine (m/z 124.0074) in the visceral adipose tissue of cachectic cancer patients in the 'Cachexia > 10% weight loss', 'Cachexia > 5–10% weight loss', and control cancer patient cohorts. The boxplot depicts the relative intensity of taurine in the visceral adipose tissue in these three patient groups, with the highest abundance observed in the 'Cachexia > 10% weight loss' group. ** $P \leq 0.01$.

different ways. In subcutaneous adipose tissue, amino acid metabolism had positive correlations with cofactor and vitamin metabolism in serum and negative correlations with lipid metabolism in muscle and carbohydrate metabolism in the liver. By contrast, visceral adipose tissue had relatively few pathway correlations with other organs. There were multiple negative correlations between carbohydrate metabolism in the liver and nucleotide metabolism in the serum, in addition to positive correlations between lipid metabolism in the liver and cofactor and vitamin metabolism in the muscle. There were also positive correlations between amino acid metabolism in serum and various metabolic pathways in subcutaneous adipose tissue. Metabolism of cofactors and vitamins in muscle was positively correlated with lipid metabolism in serum, whereas energy metabolism in muscle was negatively correlated with lipid metabolism in subcutaneous adipose tissue. By analyzing the circos plot, we identified specific pathways that are dysregulated in CCx and that may be involved in inter-organ cross-talk (Fig. 6b).

3.9. Exploring diagnostic models for cachexia classification

We applied machine learning to analyze metabolomic data from various tissues, including 5 control samples and 10 cancer cachexia samples, $n_{samples} = 75$, which encompassed the liver, muscle, visceral and subcutaneous adipose tissues, and serum. In the first step, we evaluated the ability to differentiate between cachexia and the control group within each specific organ. Organ-specific classifiers for visceral and subcutaneous adipose tissues, liver, skeletal muscle, and serum were developed using the 50 most distinguishing metabolites. The resulting classifications exhibited high accuracy, sensitivity, and specificity (Fig. 7).

In the subsequent step, we explored whether distinguishing cachexia across various organs is possible through serum metabolomics, providing a minimally invasive alternative to tissue biopsies. We compared organ-specific classifiers with serum data, creating classifiers incorporating metabolites common to both serum and the respective organ. Applying these organ-specific classifiers to serum samples allowed accurate assessment of cachexia status for individual organs (Fig. 8a–d). Overall, our findings demonstrate promising accuracy, sensitivity, and specificity of the organ-specific markers applied to serum, indicating their potential utility in diagnosing cachexia across diverse organ systems.

In the final stage, we developed a comprehensive classifier using metabolites common to serum and all other organs (liver, muscle, subcutaneous and visceral adipose tissues), which was then applied to serum samples. This classifier also performs well, albeit slightly less effectively than the individual organ-specific classifiers, revealing accuracies, sensitivities, and specificities of 0.9755, 0.9760, 0.9750 for liver; 0.8695, 0.9080, 08310 for muscle; 0.8005, 0.8140, 0.7870 for subcutaneous adipose; 0.8380, 0.8520, 0.8240 for visceral adipose; and 0.8250, 0.7960, 0.8540 for serum (Fig. 8e).

4. Discussion

In this study, for the first time, liver, muscle, subcutaneous, visceral adipose tissues, and serum from 10 cachectic and five control patients with cancer were investigated using spatial metabolomics to examine metabolic alterations associated with CCx in situ. Multiple significant differences in metabolism of cachectic compared to control patients were demonstrated. When comparing all cachexia patients with the control group, the most significant metabolic changes are observed in adipose tissue, followed by the liver, muscle, and serum. In cases of severe cachexia, there is a pronounced increase in metabolic changes in visceral adipose tissue. Pathways for carbohydrate metabolism, lipid metabolism, and metabolism of amino acids and vitamins had the most interactions across different organ systems in CCx. The liver showed the most correlations with other organs, followed by serum and muscle. Subcutaneous adipose tissue and visceral adipose tissue interacted with other organs in very different ways. Subcutaneous adipose tissue exhibited multiple pathway correlations with serum, muscle, and liver, whereas visceral adipose tissue had few pathway correlations with other organs. These findings support the concept that CCx is a multi-organ syndrome involving metabolic disturbance and altered function of multiple organ systems.

The significant metabolic alterations in visceral adipose tissue are morphologically correlated with a reduction in the cell size of adipocytes. Therefore, the metabolic and morphological findings underscore the catabolic metabolic state of these adipocytes. Most of the metabolites in subcutaneous and visceral adipose tissues were increased in patients with CCx. Subcutaneous adipose tissue was more affected by amino acid changes, whereas visceral adipose tissue was more affected by changes in lipid metabolism. Patients with CCx had increased levels of pyruvate and oxalacetate and reduced levels of fumarate in their subcutaneous adipose tissue compared with control patients. These findings are in agreement with the results of a transcriptomics study of subcutaneous adipose tissue in patients with CCx that found upregulated fatty acid degradation pathways and alterations of alanine and aspartate metabolism [36]. Under catabolic conditions, the rate of fat oxidation is increased as a result of elevated lipolysis to provide energy [36].

We observed a significant upregulation of arachidonic acid (AA) and unsaturated fatty acid metabolism in visceral adipose tissue, which plays a crucial role in the regulation of inflammation and metabolic processes in cancer cachexia [5,37]. The lipoxygenase (LOX) pathway, particularly the 5-LOX enzyme, is instrumental in the production of pro-inflammatory eicosanoids such as leukotrienes. Inhibiting LOX enzymes can reduce these eicosanoids, potentially mitigating muscle wasting and systemic inflammation observed in cancer cachexia [38,39]. This suggests that the AA-LOX pathway could be a viable therapeutic target to alleviate the inflammatory and catabolic effects of this condition. Obesity represents the other end of the spectrum of cancer cachexia. In the context of obesity, adipose tissue also exhibits increased AA metabolism, which is associated with heightened inflammation and metabolic dysfunction [40,41]. Chronic inflammation in adipose tissue is a key factor contributing to insulin resistance and

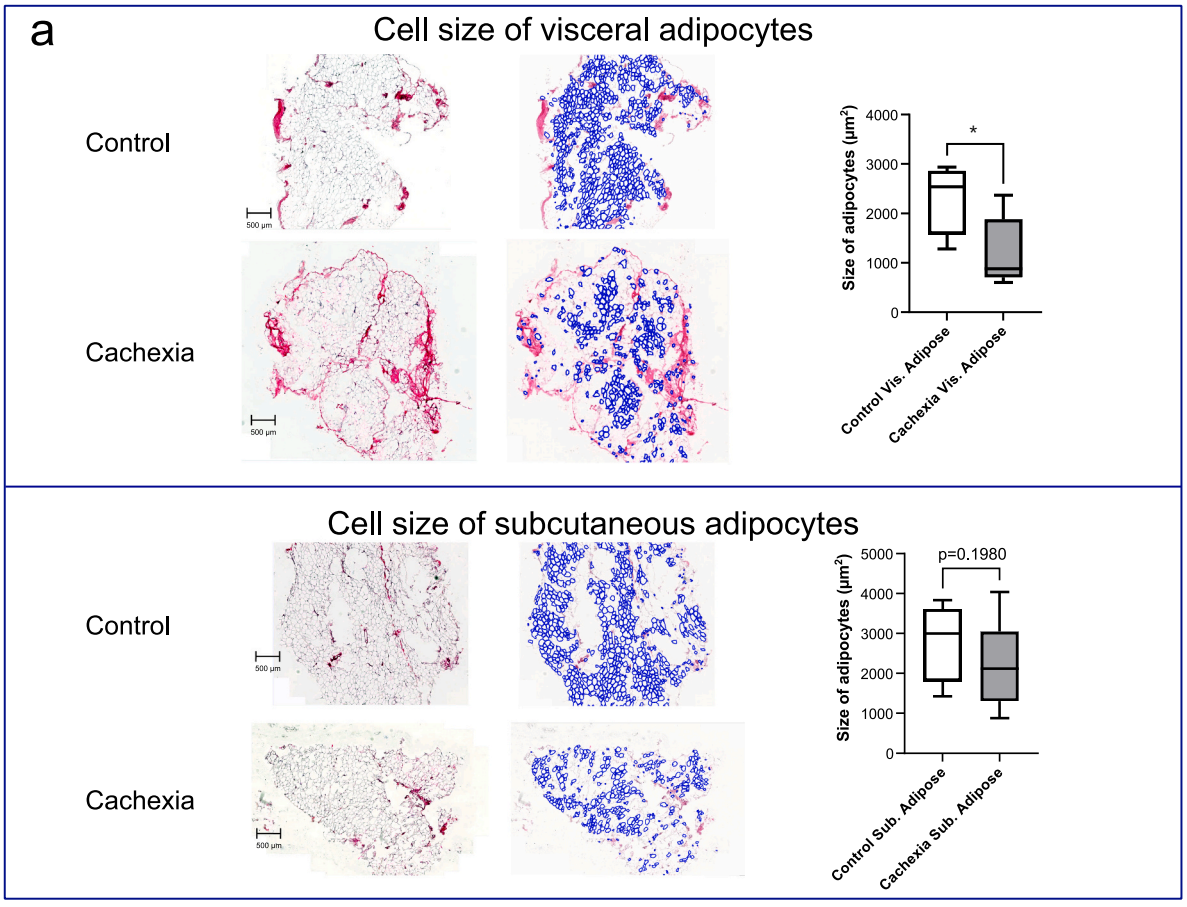

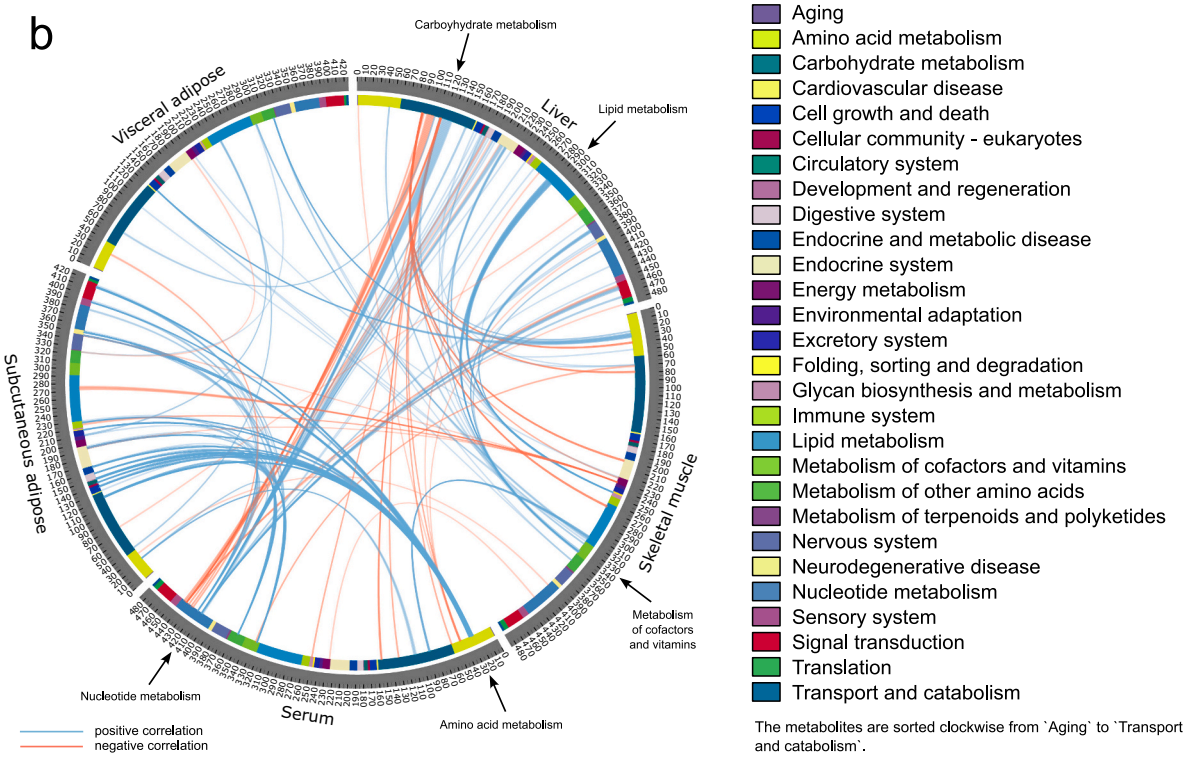

The metabolites are sorted clockwise from `Aging` to `Transport and catabolism`.

(caption on next page)

Fig. 6. Circos plot depicting inter-organ correlations among serum and liver, muscle, subcutaneous adipose, and visceral adipose tissues.
a: Image-based assessment of adipocyte size was performed on H&E-stained histological sections of visceral and subcutaneous adipose tissue obtained from both cachexia patients and the control group. Adipocyte sizes were compared using box plots. In visceral adipose tissue, adipocytes displayed a significantly smaller size compared to those in the control group. * $P \leq 0.05$.
b: The inner ring of circos plot consists of multiple color bars representing specific KEGG pathways that were enriched in multiple organs. The arcs demonstrate multi-organ correlations. Blue color means positive correlations, and red means negative correlations. The numbers in the Circos plot denote the metabolites analyzed in our study. These metabolites are organized clockwise in the plot, aligning with the sequential order of their respective metabolic pathways, spanning from pathway aging to transport and catabolism. Carbohydrate, lipid, amino acid, nucleotide and vitamin metabolism displayed correlations across organ systems in the patients with CCx. The liver exhibited the most pathway correlations with other organs. Subcutaneous adipose tissue and visceral adipose tissue interacted with other organs in very different ways. (For interpretation of the references to color in this figure legend, the reader is referred to the web version of this article.)

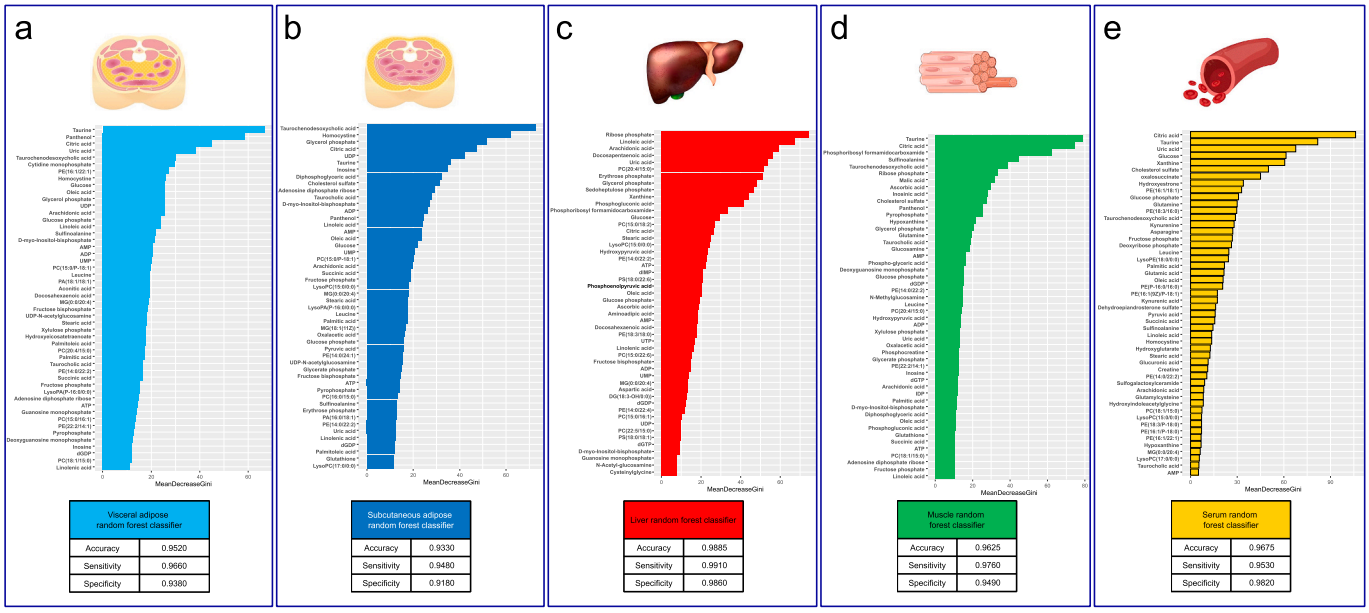

Fig. 7. Exploring diagnostic models for cachexia classification.
The feature importance of the top 50 important metabolites used for the Random Forest (RF) classifier to differentiate between the control and CCx groups were illustrated. Their corresponding accuracy, sensitivity, and specificity were listed for visceral adipose (a), subcutaneous adipose (b), liver (c), muscle (d), and serum (e), respectively. The respective m/z species of the shown metabolites are listed in Supplementary Table 3.

metabolic dysregulation in obesity. Therefore, inhibiting the LOX pathway in obesity could lower inflammation levels, thereby improving insulin sensitivity and overall metabolic health [42]. Furthermore, differential regulation of the AA metabolism pathways in cancer cachexia and obesity underscores the complexity of metabolic and inflammatory responses in these conditions. While both conditions feature elevated AA metabolism, the resultant metabolic and inflammatory outcomes differ, necessitating tailored therapeutic approaches. Our findings highlight the potential of targeting the AA-LOX pathway to modulate lipid mediator production. By reducing inflammation and improving metabolic outcomes, this strategy could offer therapeutic benefits for both cancer cachexia and obesity-related conditions. This approach aligns with the growing body of evidence supporting the role of lipid mediators in inflammation and metabolic regulation, underscoring the need for further research to elucidate the therapeutic potential of AA metabolism modulation in these conditions.

The 'browning' of adipose tissue refers to the process by which white adipocytes acquire characteristics similar to those of brown adipose tissue, resulting in several notable metabolic changes. This phenomenon is characterized by an increase in mitochondrial density, as brown adipocytes possess a higher number of mitochondria compared to white adipocytes [43]. The process also involves the upregulation of uncoupling protein 1 (UCP1) in the mitochondria of brown fat cells [44]. This protein facilitates the uncoupling of oxidative phosphorylation, causing the energy from fat burning to be released as heat instead of being used to synthesize ATP, a mechanism known as thermogenesis [43,45]. Additionally, browning stimulates lipolysis, enhancing the mobilization and breakdown of fat stores to provide fatty acids for heat generation [43,45]. Furthermore, brown adipocytes secrete a range of metabolically active molecules (adipokines) that positively affect glucose metabolism and overall energy homeostasis [5,43]. In our study, we identified elevated energy charge, increased metabolic activity, and enhanced lipolysis in adipose tissue associated with cancer cachexia (CCx). These findings suggest the presence of a browning effect. However, we did not specifically evaluate UCP1 expression through staining, which is a marker of browning. Future research should further investigate the role of adipose tissue browning in cancer cachexia to develop new strategies for mitigating its adverse effects on patients.

Variations in tryptophan metabolism, particularly through the kynurenine pathway, can significantly influence systemic metabolic processes, impacting both adipose tissue and skeletal muscle. The kynurenine pathway converts tryptophan into kynurenine, which can affect serotonin levels. Serotonin, a neurotransmitter synthesized from tryptophan, plays a critical role in mood stabilization and appetite regulation [46,47]. Altered serotonin levels can have profound effects on metabolic states and contribute to the pathophysiology of cancer cachexia [5,47]. In adipose tissue, disrupted serotonin signaling can lead to increased lipolysis and subsequent fat depletion. In skeletal muscle, impaired serotonin signaling can negatively impact protein synthesis, contributing to accelerated muscle wasting and weakness. Disruptions in serotonin levels can affect the brain's control over hunger and satiety, leading to reduced food intake and altered energy balance, which can exacerbate the cachectic state [5,48]. Understanding the interplay between altered tryptophan metabolism, serotonin signaling, and brain

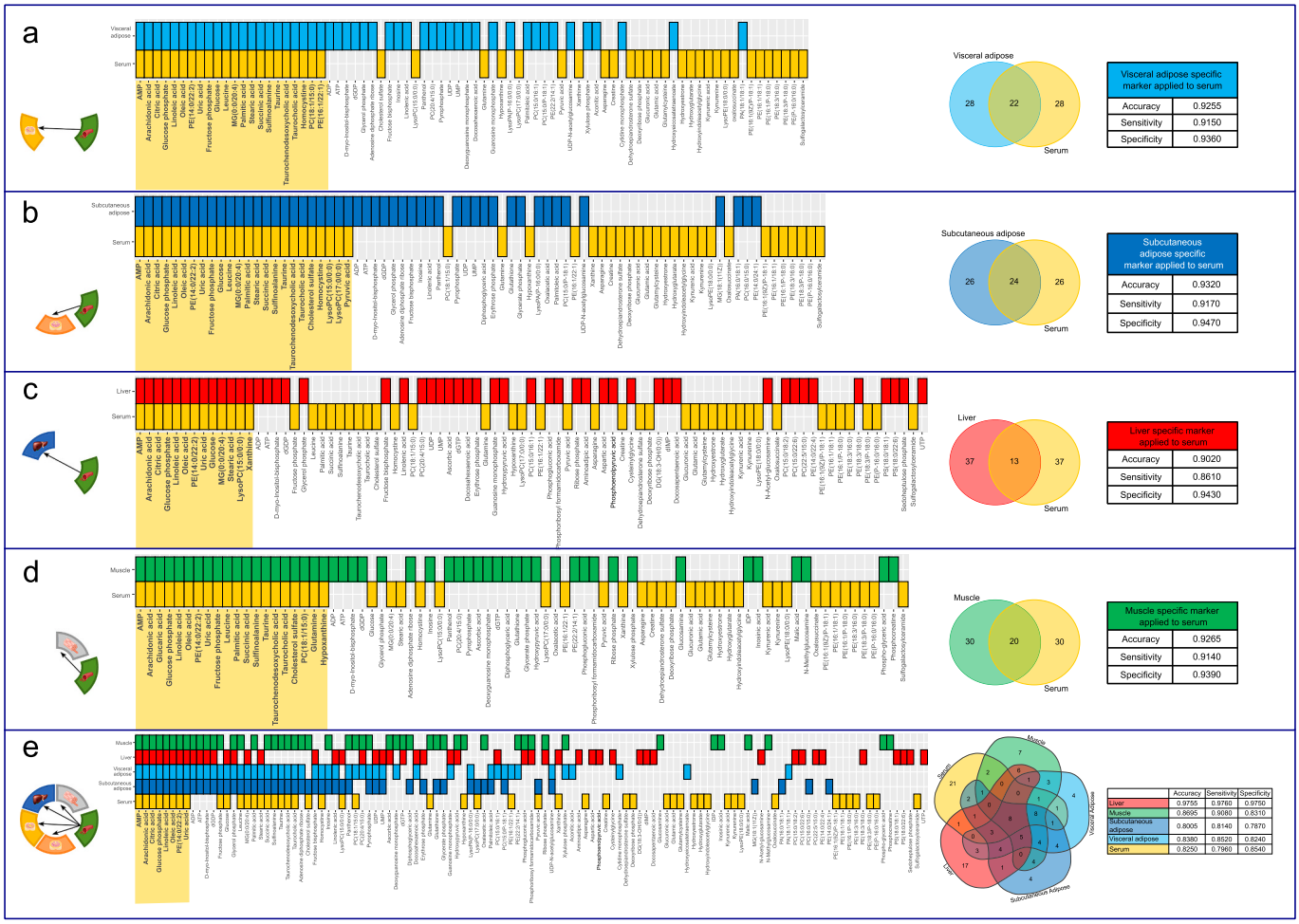

Fig. 8. Organ-specific classifiers applied to serum for cachexia classification.
Organ-specific classifiers were compared with serum, resulting in the creation of a classifier that exclusively incorporates metabolites common to both serum and the respective organ. The heatmap and Venn diagram illustrate the common metabolites found in the classifiers of serum and the respective organ: visceral adipose (a), subcutaneous adipose (b), liver (c), muscle (d), and serum (e), as well as a comprehensive classifier across both serum and all 5 multiple organs (f). The performance of the Random Forest (RF) classifier validated in serum was presented.

function highlights the complexity of cancer cachexia.

We found that the liver exhibited significant metabolic changes and correlations with other organs in CCx. The liver is thought to contribute directly to CCx by inducing hypermetabolism and increasing energy expenditure [49]. Potgens et al. reported a clear difference in the metabolic profiles of tumor-bearing mice with and without cachexia; using metabolomics data from mice with C26 tumor-induced cachexia, they found more molecules to be increased than decreased in the cachectic murine liver [50]. This is in line with our findings that more molecules were increased rather than decreased in the livers of patients with CCx compared with control patients. Our analysis of liver samples revealed significant changes in amino acid, lipid, and carbohydrate metabolism. A recent analysis of metabolomics data from cachectic C26 mice showed similar changes in lipid metabolism [51]. Morigny et al. showed that ceramide turnover in liver was the major contributor to elevated sphingolipid levels in CCx [52]. These results suggest that instead of hepatic lipid accumulation or lipotoxicity contributing to cachexia, lipid peroxidation and cellular oxidative damage might influence the uncoupling of OXPHOS in mitochondria of the cachectic liver. This might in turn contribute to increased energy expenditure and weight loss in cachexia.

We observed CCx-related changes in amino acid, lipid, and carbohydrate metabolism in skeletal muscle. These results are in line with previous findings. Der-Torossian et al. reported involvement of all three macronutrients in cachexia-related changes in gastrocnemius muscle in a colon-26 (C26) cachectic mouse model [53]. Furthermore, transcriptomics and metabolomics data from murine gastrocnemius muscle suggested that pathways for amino acid and carbohydrate metabolism are perturbed in CCx [54]. The upregulation of arginine and proline metabolism in the skeletal muscle of CCx patients in the present study is in accordance with previous observations of increased arginine and proline levels in the skeletal muscle of cachectic mice [17]. Another previous study found increased levels of asymmetric dimethyl arginine in the skeletal muscle of patients with CCx, which seemed to contribute to impaired muscle protein synthesis [55]. These findings suggest that upregulation of arginine and proline metabolism during metabolic stress in CCx impedes protein metabolism and stimulates proteolysis, leading to muscle wasting.

Energy charge (EC) reflects the balance between energy production and consumption, crucial for regulating cellular metabolism. We investigated EC in liver, muscle, and adipose tissues of cachectic patients compared to controls. Our findings reveal distinct EC levels across these tissues, with muscle and adipose tissues exhibiting higher EC compared to the liver. This discrepancy stems from the higher metabolic activity of muscle and adipose tissues, contrasting with the liver's role primarily in energy storage and metabolism. This pattern aligns with existing literature, which consistently reports lower ATP levels in the liver due to its extensive metabolic functions such as gluconeogenesis, glycogen

storage, detoxification, and lipid metabolism. In contrast, skeletal muscle maintains higher ATP levels owing to its efficient ATP production through both aerobic and anaerobic pathways, ensuring a stable energy supply during muscle contraction. Adipose tissue, primarily involved in energy storage, maintains relatively high ATP levels due to its lower metabolic rate and energy demand. Our study reveals a significant decrease in energy charge (EC) within muscle tissue affected by cancer cachexia (CCx), indicating impaired metabolic activity in these patients, consistent with previous findings [14,17]. This decline in EC correlates with specific protein breakdown, disruptions in protein turnover, mitochondrial dysfunction, and changes in substrate utilization, collectively contributing to the observed metabolic dysregulation in CCx muscle tissue [14,17]. Interestingly, liver and adipose tissues showed increased EC levels in the context of cachexia, suggesting adaptive metabolic changes in response to altered energy demands and metabolic stress. Liver tissue plays a crucial role in metabolic regulation and could be enhancing energy production to meet increased demands in cachectic states. Adipose tissue alterations in energy charge reflect shifts in lipid metabolism and energy storage mechanisms in response to systemic metabolic changes in CCx. These observations underscore the complexity of tissue-specific metabolic adaptations in cancer cachexia. Notably, the influence of hypoxia on tissue EC warrants consideration. Hypoxia-induced metabolic alterations could potentially influence EC measurements, particularly in tissues with high oxygen demand like skeletal muscle and liver. Future research should explore the molecular mechanisms underlying these tissue-specific responses to deepen our understanding of their implications for disease progression and therapeutic strategies.

As CCx is seen as a multi-organ syndrome, it was hypothesized that mediators released from various tissues might be directly involved in the generation of the main metabolic alterations in CCx [1]. Organs such as muscle, adipose tissue, and liver may also play an important role in the progression of CCx by exacerbating the pro- and anti-inflammatory responses initially activated by the tumor and the immune system [56]. Argiles et al. reported that abnormalities associated with CCx include alterations in carbohydrate, lipid, and protein metabolism as well as anorexia, insulin resistance, and increased muscle protein degradation [1,57]. We found indirect evidence that the liver communicates strongly with other organs, whereas serum, muscle, and adipose tissue do so less strongly. We also found that subcutaneous adipose tissue and visceral adipose tissue interact with other organs in very different ways. Carbohydrate metabolism, lipid metabolism, and amino acid and vitamin metabolism were the metabolic pathways with the most interactions across different organ systems in patients with CCx. Our results suggest a complex and still poorly understood inter-organ crosstalk in CCx; however, future studies are needed to uncover the molecular mechanisms of this crosstalk.

We also emphasized nucleotide metabolism, an area of notable interest in the study of cancer cachexia (CCx). Previous studies, such as those by Lautaoja et al. [58], have observed changes in nucleotide and amino acid metabolism in mouse models of cachexia, further underscoring the relevance of these pathways in CCx. Similarly, research by Rohm et al. (2019) highlighted alterations in nucleotide metabolism in cachectic mice, indicating its role in muscle wasting and energy imbalance [59]. In our study, network analysis clearly indicates that nucleotide metabolism, amino acid metabolism, and arachidonic acid metabolism are significantly upregulated in CCx liver compared to control patients. This upregulation contributes significantly to the metabolic changes in CCx, as evidenced by the prominent role of nucleotide metabolism in the circus plot. Notably, nucleotide metabolism's influence extends beyond isolated pathways, suggesting a systemic impact on overall metabolic homeostasis. Moreover, we identified multiple negative correlations between carbohydrate metabolism in the liver and nucleotide metabolism in the serum. This finding suggests intricate regulatory mechanisms and compensatory responses in the body's attempt to maintain metabolic balance under cachexia conditions. These complex interactions underscore the critical role of nucleotide metabolism within the broader metabolic network affected by CCx. The significance of nucleotide metabolism in CCx is also supported by studies indicating its involvement in inflammation and immune responses, key components of cachexia pathophysiology [1,22]. Altered nucleotide metabolism can influence cellular energy status, signal transduction, and gene expression, all of which are vital for maintaining muscle and liver function during cachexia.

Our extensive datasets, gathered from various organ systems in cancer patients with and without cancer cachexia, reveal significant metabolic differences. These datasets are valuable for diagnostic classification through machine learning, effectively distinguishing cachexia within specific organs such as the liver, muscle, and adipose tissue. However, organ-specific differentiation, which relies on invasive and ethically complex biopsies, has limited practical utility for developing biomarkers. To overcome this challenge, we explored the potential to differentiate cachexia across organs using serum metabolomics, offering a simple alternative to tissue biopsies. For the first time, we compared organ-specific classifiers with serum data and developed classifiers that combine metabolites shared between serum and respective organs. Applying this organ-specific classifier to serum enables effective evaluation of cachexia in individual organs. Additionally, we created a versatile classifier containing metabolites common to serum and all other organs. While not as potent as individual organ-specific classifiers, this comprehensive classifier enables a clear distinction of CCx. Examination of these classifiers identified metabolites with the highest Gini importance, revealing distinctive patterns representing key metabolic pathways, including glucose metabolism, the tricarboxylic acid cycle, purine metabolism, amino acid metabolism, and lipid metabolism. These key metabolites serve as surrogates for essential metabolic pathways altered in cancer cachexia, explaining the effective differentiation between cachexia and control groups. The selection of AMP, arachidonic acid, citric acid, glucose phosphate, phosphatidylethanolamine, oleic acid, and uric acid for the joint classifier distinguishing serum from all organs is attributed to their potential synergistic effects in reflecting the complex metabolic alterations associated with cachexia. AMP serves as a crucial indicator of energy metabolism, while arachidonic acid, a precursor to inflammatory eicosanoids, reflects tissue inflammation and metabolic dysregulation in cachectic states [60]. Citric acid, pivotal in the citric acid cycle, alongside glucose phosphate, the primary energy substrate, indicate systemic metabolic shifts and energy production changes observed in cachexia [22]. Phosphatidylethanolamines, essential in cell membrane integrity and signaling, may reflect tissue-specific alterations in lipid metabolism, with oleic acid, a monounsaturated fatty acid, contributing to lipid homeostasis disturbances characteristic of cachectic conditions. Uric acid, the endpoint of purine metabolism, mirrors metabolic stress and inflammation in tissues affected by cachexia [61]. Together, these metabolites provide a comprehensive view of the multifactorial nature of cachexia, leveraging their combined metabolic and biological roles to distinguish between cachectic and control states with greater sensitivity and specificity. Their synergistic interactions in reflecting diverse aspects of metabolic dysfunction and tissue inflammation underscore their utility in the classifier model aimed at non-invasive diagnosis and understanding of cachexia.

The identified metabolic changes across liver, muscle, adipose tissues, and serum in CCx underscore the multi-organ involvement and complex metabolic dysregulation characterizing this syndrome. Therapeutically, targeting these metabolic pathways could potentially mitigate the progression of cachexia. For instance, strategies aimed at restoring amino acid balance, regulating lipid metabolism, and enhancing energy utilization pathways in affected tissues may attenuate muscle wasting and metabolic stress associated with CCx [15,62]. Furthermore, understanding the role of nucleotide metabolism and its interactions with other metabolic pathways could offer novel therapeutic targets, potentially influencing inflammation and immune responses crucial to cachexia pathophysiology [14]. Integrating these

insights with advanced diagnostic approaches, such as serum metabolomics-based classifiers, could facilitate early detection and personalized treatment strategies for patients with CCx, emphasizing the importance of multi-omics research in advancing therapeutic interventions.

The brain plays a crucial role in the pathophysiology of cancer cachexia by integrating and responding to systemic metabolic changes occurring in the liver, skeletal muscle, and adipose tissue. This central integration affects the overall progression of cachexia and its manifestations across these organs [5,63]. In the liver, cancer cachexia disrupts glucose and lipid metabolism. The brain monitors these changes through circulating metabolites and hormones, and impaired liver function contributes to systemic insulin resistance, affecting brain energy regulation. The liver also produces inflammatory cytokines in response to systemic inflammation, which can cross the blood-brain barrier, leading to neuroinflammation and influencing appetite and energy expenditure [64,65]. In skeletal muscle, cachexia leads to significant muscle wasting due to increased protein breakdown and decreased synthesis. The brain responds to signals of muscle loss by altering appetite and energy balance. Muscle-derived myokines, which are altered in cachexia, affect brain signaling related to muscle mass and physical function, potentially worsening fatigue and cognitive impairment. In adipose tissue, the loss of fat mass in cachexia alters the production of adipokines like leptin and adiponectin. These changes disrupt the brain's regulation of appetite and energy expenditure, contributing to further weight loss and metabolic imbalance [63]. Inflammation in adipose tissue releases mediators that can impact brain function, influencing systemic inflammation and the progression of cachexia. Overall, the brain regulates appetite and energy expenditure through complex feedback systems involving peripheral metabolic signals. Disruptions in these systems during cancer cachexia lead to decreased food intake, increased energy expenditure, fatigue, and cognitive impairments, which exacerbate the condition [5,46,63]. Understanding these interactions is crucial for developing targeted interventions to manage cancer cachexia effectively and improve patient outcomes.

5. Strengths and weaknesses

This study is the first to employ spatial metabolomics to investigate multiple organs from cachectic and control cancer patients, offering a comprehensive and detailed analysis of cancer cachexia (CCx). By analyzing multiple tissues simultaneously, the study underscores the systemic nature of CCx and sheds light on inter-organ cross-talk and metabolic interactions. The identification of significant metabolic pathway alterations, coupled with advanced techniques such as pathway enrichment and correlation network analyses, deepens our understanding of CCx pathophysiology. Our approach of integrating organ-specific metabolic classifiers into serum samples from cancer cachexia patients represents a significant advancement in the development of classifiers for potential diagnostic biomarkers using machine learning techniques.

However, it's essential to note that these findings are preliminary and limited due to the small dataset of 75 tissue samples and the absence of an independent validation cohort. In the next phase, it is of great interest to validate and, more importantly, refine these classifiers using larger and statistically robust cohorts through artificial intelligence and machine learning. The comparison of metabolites between the CCx and control groups did not include P-value corrections to align with our discovery-oriented study's goal of maximizing sensitivity to identify potential associations and generate hypotheses. Additionally, we validated our findings through spatial two-dimensional visualization of metabolites and further confirmed them using machine learning and principal component analysis. Our study provides a snapshot of each patient at a single time point and does not take into account dynamic changes over time. Further studies should be designed as longitudinal studies to validate our findings. It is important to clarify that our study primarily focused on the metabolic consequences of cancer cachexia rather than on the direct analysis of tumor growth dynamics. The observed changes reflect the metabolic alterations associated with the systemic effects of cancer cachexia and provide valuable insights into pathways potentially relevant to cancer cachexia in humans.

Moreover, comparative analyses across different metabolic states, including healthy controls and obese groups, would deepen our understanding of metabolic differences and similarities. Cancer cachexia and obesity represent two extremes of metabolic dysregulation, and comparing these conditions can help identify overlapping metabolic pathways. This approach could also highlight specific biomarkers and therapeutic targets relevant to both conditions, potentially improving clinical outcomes. For instance, our findings reveal overlapping metabolic disturbances in arachidonic acid metabolism between cancer cachexia and obesity. This indicates that further research into these shared pathways could uncover new therapeutic aspects and strategies for managing both conditions effectively.

6. Conclusions

In summary, we conducted a multi-organ metabolomics study using spatial metabolomics in human patients with CCx. The results reveal multiple changes in metabolic pathways across organs, indicating various interactions. Our analysis suggests a close interaction between liver and adipose tissue in CCx, whereas interactions involving muscle metabolism were less pronounced. These interactions should be investigated in more detail in the future to gain a better understanding of cachexia. The classification models demonstrate that achieving effective differentiation at the organ level is feasible, and obtaining distinction in serum regarding cachexia status at the organ level is also possible. This tissue-based approach has been undertaken in this study for the first time, suggesting its potential for further development and application in larger patient cohorts.

7. Translation potential

This study significantly advances the understanding of cancer cachexia by illustrating the multi-organ nature of the syndrome and identifying distinct metabolic alterations across various tissues. The integration of spatial metabolomics and machine learning opens new avenues for diagnosing and monitoring CCx. The development of serum-based classifiers holds significant translational potential by providing a less invasive alternative to tissue biopsies. These classifiers could facilitate the monitoring of CCx progression and treatment response in clinical practice. Additionally, serum-based classifiers can be used for identifying patients at higher risk of developing CCx, necessitating more intensive monitoring. Future research should focus on validating these findings in larger cohorts and exploring longitudinal studies to capture the dynamic changes in CCx. The study's approach and findings contribute to the development of therapeutic strategies targeting the metabolic dysregulation in CCx, ultimately improving patient outcomes.

Supplementary data to this article can be found online at https://doi.org/10.1016/j.metabol.2024.156034.

Funding

The study was funded by the Ministry of Education and Research of the Federal Republic of Germany (BMBF; Grant Nos. 01ZX1610B and 01KT1615), the "Deutsche Forschungsgemeinschaft" (Grant Nos. SFB 824TP C04 and CRC/Transregio 205/1) to A.W. and N.S., and the Else Kröner-Fresenius-foundation, Bad Homburg, to H.H. and M.C.. O.P. was supported by a Clinical Leave Stipend from the German Center of Infection Research (DZIF, grant TI07.001). This work is supported by the Novo Nordisk Foundation (NNF21SA0072102, NIDDK UM1 557 DK126185, NIDDK DK102173).

CRediT authorship contribution statement

Na Sun: Writing – review & editing, Writing – original draft, Visualization, Validation, Methodology, Investigation, Formal analysis, Data curation. **Tanja Krauss:** Writing – review & editing, Writing – original draft, Visualization, Validation, Methodology, Investigation, Formal analysis, Data curation. **Claudine Seeliger:** Writing – review & editing, Writing – original draft, Validation, Investigation, Formal analysis, Data curation. **Thomas Kunzke:** Writing – review & editing, Visualization, Methodology, Formal analysis, Data curation. **Barbara Stöckl:** Writing – review & editing, Visualization, Methodology, Formal analysis, Data curation. **Annette Feuchtinger:** Writing – review & editing, Visualization, Software, Methodology, Investigation, Formal analysis, Data curation. **Chaoyang Zhang:** Writing – review & editing, Software, Methodology, Formal analysis. **Andreas Voss:** Writing – review & editing, Visualization, Formal analysis. **Simone Heisz:** Writing – review & editing, Resources, Methodology, Data curation. **Olga Prokopchuk:** Writing – review & editing, Validation, Resources, Methodology, Investigation, Funding acquisition, Data curation. **Marc E. Martignoni:** Writing – review & editing, Resources, Methodology, Investigation, Data curation. **Klaus-Peter Janssen:** Writing – review & editing, Visualization, Validation, Resources, Methodology, Investigation, Data curation. **Melina Claussnitzer:** Writing – review & editing, Visualization, Validation, Supervision, Resources, Project administration, Methodology, Investigation, Funding acquisition, Data curation, Conceptualization. **Hans Hauner:** Writing – review & editing, Writing – original draft, Visualization, Validation, Supervision, Resources, Project administration, Methodology, Investigation, Funding acquisition, Formal analysis, Data curation, Conceptualization. **Axel Walch:** Writing – review & editing, Writing – original draft, Visualization, Validation, Supervision, Resources, Project administration, Methodology, Investigation, Funding acquisition, Formal analysis, Data curation, Conceptualization.

Declaration of competing interest

The authors declare no competing financial interests.

Data availability

The imaging mass spectrometry data for liver, muscle, visceral adipose tissue, subcutaneous adipose tissue, and serum are available on Mendeley Data at the following link: https://data.mendeley.com/datasets/f8s7r2sf9t/1 [66].

Acknowledgements

The authors certify that they comply with the ethical guidelines for publishing in *Metabolism*.

References

[1] Argilés JM, et al. Cancer cachexia: understanding the molecular basis. Nat Rev Cancer 2014;14(11):754–62. https://doi.org/10.1038/nrc3829.
[2] Haehling S, Anker SD. Cachexia as a major underestimated and unmet medical need: facts and numbers. J Cachexia Sarcopenia Muscle 2010;1(1):1–5. https://doi.org/10.1007/s13539-010-0002-6.
[3] Baracos VE, et al. Cancer-associated cachexia. Nat Rev Dis Primers 2018;4:17105. https://doi.org/10.1038/nrdp.2017.105.
[4] Cao Z, et al. Biomarkers for cancer cachexia: a mini review. Int J Mol Sci 2021;22(9). https://doi.org/10.3390/ijms22094501.
[5] Argiles JM, et al. Inter-tissue communication in cancer cachexia. Nat Rev Endocrinol 2018;15(1):9–20. https://doi.org/10.1038/s41574-018-0123-0.
[6] Han J, et al. Imaging modalities for diagnosis and monitoring of cancer cachexia. EJNMMI Res 2021;11(1):94. https://doi.org/10.1186/s13550-021-00834-2.
[7] Schmidt SF, et al. Cancer cachexia: more than skeletal muscle wasting. Trends Cancer 2018;4(12):849–60. https://doi.org/10.1016/j.trecan.2018.10.001.
[8] Biswas AK, Acharyya S. Understanding cachexia in the context of metastatic progression. Nat Rev Cancer 2020;20(5):274–84. https://doi.org/10.1038/s41568-020-0251-4.
[9] Gallagher IJ, et al. Omics/systems biology and cancer cachexia. Semin Cell Dev Biol 2016;54:92–103. https://doi.org/10.1016/j.semcdb.2015.12.022.
[10] O'Connell TM, et al. Metabolic biomarkers for the early detection of cancer cachexia. Front Cell Dev Biol 2021;9:720096. https://doi.org/10.3389/fcell.2021.720096.
[11] Khamoui AV, et al. Aerobic and resistance training dependent skeletal muscle plasticity in the colon-26 murine model of cancer cachexia. Metabolism 2016;65(5):685–98. https://doi.org/10.1016/j.metabol.2016.01.014.
[12] Cala MP, et al. Multiplatform plasma fingerprinting in cancer cachexia: a pilot observational and translational study. J Cachexia Sarcopenia Muscle 2018;9(2):348–57. https://doi.org/10.1002/jcsm.12270.
[13] Miller J, et al. Plasma metabolomics identifies lipid and amino acid markers of weight loss in patients with upper gastrointestinal cancer. Cancers 2019;11(10). https://doi.org/10.3390/cancers11101594.
[14] Beltra M, et al. NAD(+) repletion with niacin counteracts cancer cachexia. Nat Commun 2023;14(1):1849. https://doi.org/10.1038/s41467-023-37595-6.
[15] Cui P, et al. Metabolomics-driven discovery of therapeutic targets for cancer cachexia. J Cachexia Sarcopenia Muscle 2024;15(3):781–93. https://doi.org/10.1002/jcsm.13465.
[16] Jeevanandam M, et al. Cancer cachexia and the rate of whole body lipolysis in man. Metabolism 1986;35(4):304–10. https://doi.org/10.1016/0026-0495(86)90145-9.
[17] Kunzke T, et al. Derangements of amino acids in cachectic skeletal muscle are caused by mitochondrial dysfunction. J Cachexia Sarcopenia Muscle 2020;11(1):226–40. https://doi.org/10.1002/jcsm.12498.
[18] Cao J, et al. Mass spectrometry imaging of L-ring-13C6-labeled phenylalanine and tyrosine kinetics in non-small cell lung carcinoma. Cancer Metab 2021;9(1):26. https://doi.org/10.1186/s40170-021-00262-9.
[19] Atkinson DE. Energy charge of the adenylate pool as a regulatory parameter. Interaction with feedback modifiers. Biochemistry 1968;7(11):4030–4. https://doi.org/10.1021/bi00851a033.
[20] Prado CM, et al. Prevalence and clinical implications of sarcopenic obesity in patients with solid tumours of the respiratory and gastrointestinal tracts: a population-based study. Lancet Oncol 2008;9(7):629–35. https://doi.org/10.1016/S1470-2045(08)70153-0.
[21] Prokopchuk O, et al. A novel tissue inhibitor of metalloproteinases-1/liver/cachexia score predicts prognosis of gastrointestinal cancer patients. J Cachexia Sarcopenia Muscle 2021;12(2):378–92. https://doi.org/10.1002/jcsm.12680.
[22] Fearon K, et al. Definition and classification of cancer cachexia: an international consensus. Lancet Oncol 2011;12(5):489–95. https://doi.org/10.1016/S1470-2045(10)70218-7.
[23] Bachmann J, et al. Cachexia in patients with chronic pancreatitis and pancreatic cancer: impact on survival and outcome. Nutr Cancer 2013;65(6):827–33. https://doi.org/10.1080/01635581.2013.804580.
[24] Wang Q, et al. A simple preparation step to remove excess liquid lipids in white adipose tissue enabling improved detection of metabolites via MALDI-FTICR imaging MS. Histochem Cell Biol 2022;157(5):595–605. https://doi.org/10.1007/s00418-022-02088-y.
[25] Miura D, et al. Highly sensitive matrix-assisted laser desorption ionization-mass spectrometry for high-throughput metabolic profiling. Anal Chem 2010;82(2):498–504. https://doi.org/10.1021/ac901083a.
[26] Edwards JL, Kennedy RT. Metabolomic analysis of eukaryotic tissue and prokaryotes using negative mode MALDI time-of-flight mass spectrometry. Anal Chem 2005;77(7):2201–9. https://doi.org/10.1021/ac048323r.
[27] Aichler M, et al. N-acyl taurines and acylcarnitines cause an imbalance in insulin synthesis and secretion provoking beta cell dysfunction in type 2 diabetes. Cell Metab 2017;25(6). https://doi.org/10.1016/j.cmet.2017.04.012. p. 1334-1347 e4.
[28] Ly A, et al. High-mass-resolution MALDI mass spectrometry imaging of metabolites from formalin-fixed paraffin-embedded tissue. Nat Protoc 2016;11(8):1428–43. https://doi.org/10.1038/nprot.2016.081.
[29] Prade VM, et al. De novo discovery of metabolic heterogeneity with immunophenotype-guided imaging mass spectrometry. Mol Metab 2020;36:100953. https://doi.org/10.1016/j.molmet.2020.01.017.
[30] Wishart DS, et al. HMDB 4.0: the human metabolome database for 2018. Nucleic Acids Res 2018;46(D1):D608–17. https://doi.org/10.1093/nar/gkx1089.
[31] Palmer A, et al. FDR-controlled metabolite annotation for high-resolution imaging mass spectrometry. Nat Methods 2017;14(1):57–60. https://doi.org/10.1038/nmeth.4072.
[32] Kanehisa M, Goto S. KEGG: Kyoto encyclopedia of genes and genomes. Nucleic Acids Res 2000;28(1):27–30. https://doi.org/10.1093/nar/28.1.27.
[33] Shannon P, et al. Cytoscape: a software environment for integrated models of biomolecular interaction networks. Genome Res 2003;13(11):2498–504.
[34] Quarta C, et al. GLP-1-mediated delivery of tesaglitazar improves obesity and glucose metabolism in male mice. Nat Metab 2022;4(8):1071–83. https://doi.org/10.1038/s42255-022-00617-6.
[35] Georgiadi A, et al. Orphan GPR116 mediates the insulin sensitizing effects of the hepatokine FNDC4 in adipose tissue. Nat Commun 2021;12(1):2999. https://doi.org/10.1038/s41467-021-22579-1.
[36] Dahlman I, et al. Adipose tissue pathways involved in weight loss of cancer cachexia. Br J Cancer 2010;102(10):1541–8. https://doi.org/10.1038/sj.bjc.6605665.
[37] Petruzzelli M, Wagner EF. Mechanisms of metabolic dysfunction in cancer-associated cachexia. Genes Dev 2016;30(5):489–501. https://doi.org/10.1101/gad.276733.115.
[38] Balkwill F, Mantovani A. Inflammation and cancer: back to Virchow? Lancet 2001;357(9255):539–45. https://doi.org/10.1016/S0140-6736(00)04046-0.

[39] Ross JA, Fearon KC. Eicosanoid-dependent cancer cachexia and wasting. Curr Opin Clin Nutr Metab Care 2002;5(3):241–8. https://doi.org/10.1097/00075197-200205000-00002.
[40] Gregor MF, Hotamisligil GS. Inflammatory mechanisms in obesity. Annu Rev Immunol 2011;29:415–45. https://doi.org/10.1146/annurev-immunol-031210-101322.
[41] Hotamisligil GS. Inflammation and metabolic disorders. Nature 2006;444(7121):860–7. https://doi.org/10.1038/nature05485.
[42] Schleh MW, et al. Metaflammation in obesity and its therapeutic targeting. Sci Transl Med 2023;15(723):eadf9382. https://doi.org/10.1126/scitranslmed.adf9382.
[43] Dong M, et al. Role of brown adipose tissue in metabolic syndrome, aging, and cancer cachexia. Front Med 2018;12(2):130–8. https://doi.org/10.1007/s11684-017-0555-2.
[44] Barbatelli G, et al. The emergence of cold-induced brown adipocytes in mouse white fat depots is determined predominantly by white to brown adipocyte transdifferentiation. Am J Physiol Endocrinol Metab 2010;298(6):E1244–53. https://doi.org/10.1152/ajpendo.00600.2009.
[45] Cannon B, Nedergaard J. Brown adipose tissue: function and physiological significance. Physiol Rev 2004;84(1):277–359. https://doi.org/10.1152/physrev.00015.2003.
[46] Dwarkasing JT, et al. Increased hypothalamic serotonin turnover in inflammation-induced anorexia. BMC Neurosci 2016;17(1):26. https://doi.org/10.1186/s12868-016-0260-0.
[47] Dwarkasing JT, et al. Differences in food intake of tumour-bearing cachectic mice are associated with hypothalamic serotonin signalling. J Cachexia Sarcopenia Muscle 2015;6(1):84–94. https://doi.org/10.1002/jcsm.12008.
[48] Molfino A, et al. Cancer anorexia: hypothalamic activity and its association with inflammation and appetite-regulating peptides in lung cancer. J Cachexia Sarcopenia Muscle 2017;8(1):40–7. https://doi.org/10.1002/jcsm.12156.
[49] Porporato PE. Understanding cachexia as a cancer metabolism syndrome. Oncogenesis 2016;5:e200. https://doi.org/10.1038/oncsis.2016.3.
[50] Potgens SA, et al. Multi-compartment metabolomics and metagenomics reveal major hepatic and intestinal disturbances in cancer cachectic mice. J Cachexia Sarcopenia Muscle 2021;12(2):456–75. https://doi.org/10.1002/jcsm.12684.
[51] Khamoui AV, et al. Hepatic proteome analysis reveals altered mitochondrial metabolism and suppressed acyl-CoA synthetase-1 in colon-26 tumor-induced cachexia. Physiol Genomics 2020;52(5):203–16. https://doi.org/10.1152/physiolgenomics.00124.2019.
[52] Morigny P, et al. High levels of modified ceramides are a defining feature of murine and human cancer cachexia. J Cachexia Sarcopenia Muscle 2020;11(6):1459–75. https://doi.org/10.1002/jcsm.12626.
[53] Der-Torossian H, et al. Cancer cachexia's metabolic signature in a murine model confirms a distinct entity. Metabolomics 2013;9(3):730–9. https://doi.org/10.1007/s11306-012-0485-6.
[54] Cui P, et al. Metabolic profiling of tumors, sera, and skeletal muscles from an orthotopic murine model of gastric cancer associated-cachexia. J Proteome Res 2019;18(4):1880–92. https://doi.org/10.1021/acs.jproteome.9b00088.
[55] Kunz HE, et al. Methylarginine metabolites are associated with attenuated muscle protein synthesis in cancer-associated muscle wasting. J Biol Chem 2020;295(51):17441–59. https://doi.org/10.1074/jbc.RA120.014884.
[56] Fonseca G, et al. Cancer cachexia and related metabolic dysfunction. Int J Mol Sci 2020;21(7). https://doi.org/10.3390/ijms21072321.
[57] Argiles JM, et al. Targets in clinical oncology: the metabolic environment of the patient. Front Biosci 2007;12:3024–51. https://doi.org/10.2741/2293.
[58] Lautaoja JH, et al. Muscle and serum metabolomes are dysregulated in colon-26 tumor-bearing mice despite amelioration of cachexia with activin receptor type 2B ligand blockade. Am J Physiol Endocrinol Metab 2019;316(5):E852–65. https://doi.org/10.1152/ajpendo.00526.2018.
[59] Rohm M, et al. Energy metabolism in cachexia. EMBO Rep 2019;20:4. https://doi.org/10.15252/embr.201847258.
[60] Calder PC. Polyunsaturated fatty acids and inflammation. Prostaglandins Leukot Essent Fatty Acids 2006;75(3):197–202. https://doi.org/10.1016/j.plefa.2006.05.012.
[61] Johnson RJ, et al. Is there a pathogenetic role for uric acid in hypertension and cardiovascular and renal disease? Hypertension 2003;41(6):1183–90. https://doi.org/10.1161/01.HYP.0000069700.62727.C5.
[62] Arneson-Wissink PC, Doles JD. Disrupted NOS2 metabolism drives myoblast response to wasting-associated cytokines. Exp Cell Res 2021;407(1):112779. https://doi.org/10.1016/j.yexcr.2021.112779.
[63] Burfeind KG, Michaelis KA, Marks DL. The central role of hypothalamic inflammation in the acute illness response and cachexia. Semin Cell Dev Biol 2016;54:42–52. https://doi.org/10.1016/j.semcdb.2015.10.038.
[64] Solheim TS, et al. Is there a genetic cause of appetite loss?-an explorative study in 1,853 cancer patients. J Cachexia Sarcopenia Muscle 2012;3(3):191–8. https://doi.org/10.1007/s13539-012-0064-8.
[65] van Norren K, Dwarkasing JT, Witkamp RF. The role of hypothalamic inflammation, the hypothalamic-pituitary-adrenal axis and serotonin in the cancer anorexia-cachexia syndrome. Curr Opin Clin Nutr Metab Care 2017;20(5):396–401. https://doi.org/10.1097/MCO.0000000000000401.
[66] Sun N, et al. Imaging mass spectrometry data for liver, muscle, visceral adipose tissue, subcutaneous adipose tissue, and serum. Mendeley Data 2024;V1. https://doi.org/10.17632/f8s7r2sf9t.1.